

Mimicking the Bosonic Su-Schrieffer-Heeger model with a lattice of rings

Phys. Rev. A 108, 023317 (2023)



E. Nicolau



A. M. Marques



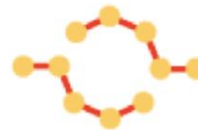
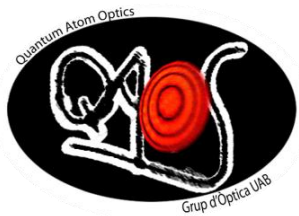
J. Mompart



R. G. Dias



V. Ahufinger



**Quantum
Transport**



Ring potentials

+

Su-Schrieffer-Heeger (SSH) model

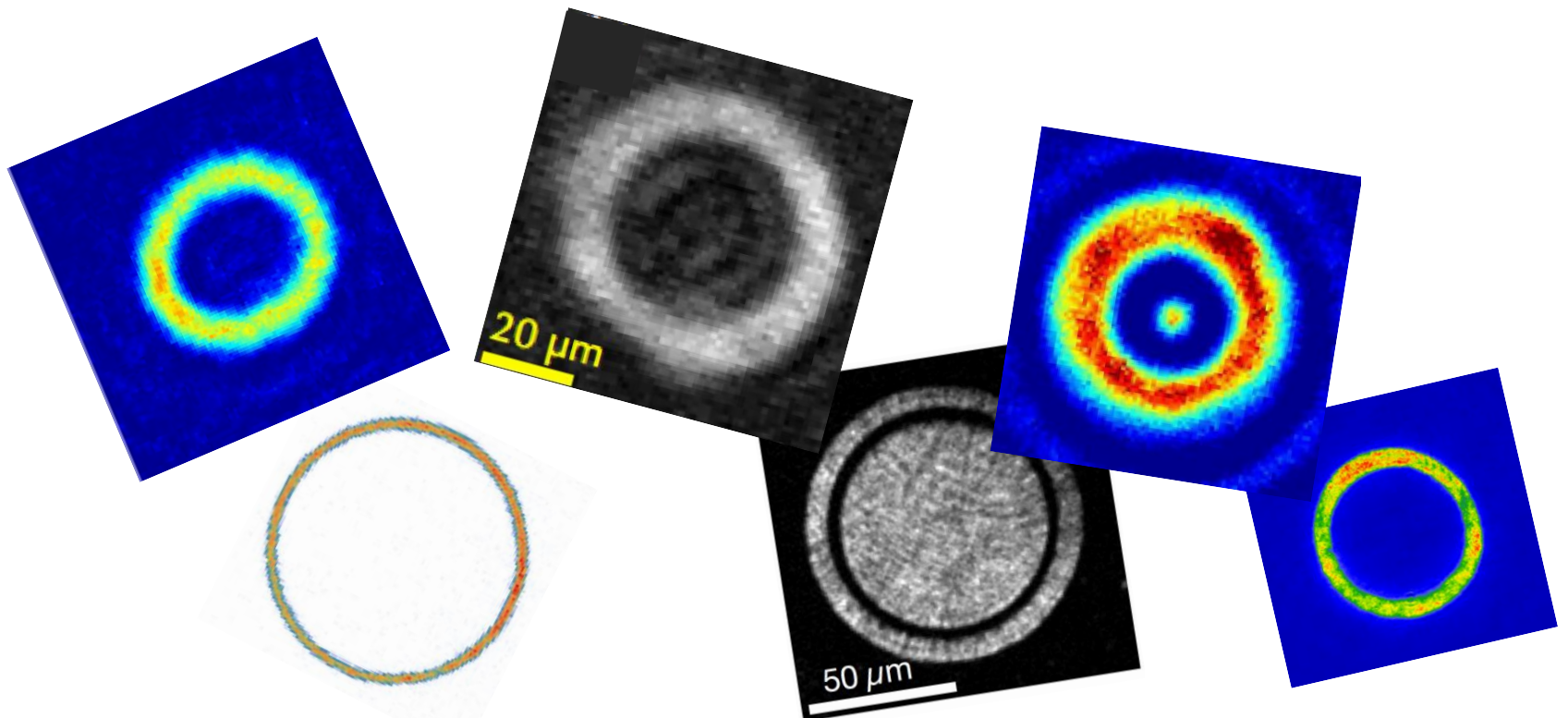


Bosonic orbital SSH in a lattice of rings

Ring potentials



Ring potentials



L. Amico *et al.*, AVS Quantum Sci. **3**, 039201 (2021).
L. Amico *et al.*, Rev. Mod. Phys. **94**, 041001 (2022).

Ring potentials

OAM transfer

Light beams

M. Andersen *et al.*, Physical Review Letters **97**, 170406 (2006).

S. Franke-Arnold, Philosophical Transactions Mathematical Physical & Engineering Sciences **375**, 20150435 (2017).

Weak link rotation

A. Ramanathan *et al.*, Physical Review Letters **106**, 130401 (2011).

K. C. Wright *et al.*, Physical Review Letters **110**, 025302 (2013).

Temperature quench

L. Corman *et al.*, Physical Review Letters **113**, 135302 (2014).

Alternatively

p band of a conventional optical lattice

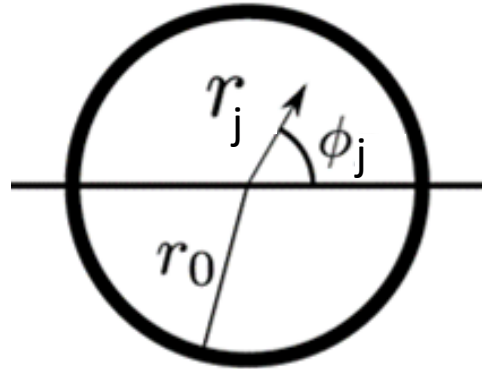
G. Wirth M. Ölschläger, and A. Hemmerich, Nature Physics **7**, 147 (2011).

X. Li and W. V. Liu, Reports on Progress in Physics **79**, 116401 (2016).

A. Kiely *et al.*, J. of Phys. B: Atomic, Molecular and Optical Physics **49**, 215003 (2016).

T. Kock *et al.*, J. of Phys. B: Atomic, Molecular and Optical Physics **49**, 042001 (2016).

Ring potentials



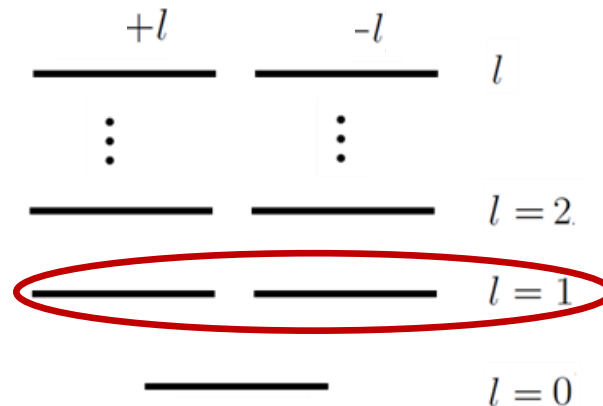
winding number, $n=\pm l$, l being the orbital angular momentum quantum number

$$\Psi_j^n(r_j, \phi_j) = \langle \vec{r} | j, n \rangle = \psi(r_j) e^{in(\phi_j - \phi_0)}$$

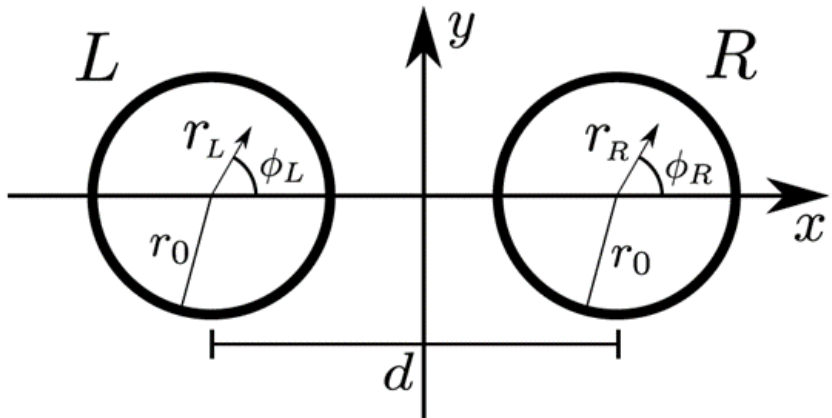
↓ ↓ ↓

index of the ring radial part phase origin

$$E = E_0 + E_c l^2$$



Ring potentials

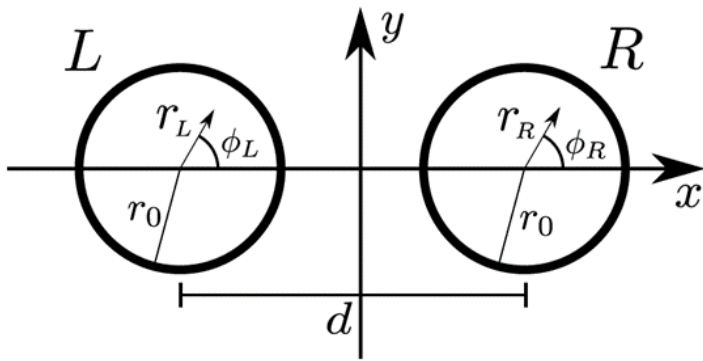


$$J_{j,n}^{k,n'} = e^{i(n-n')\phi_0} \int d^2r \Psi_{j,n}(\phi_0 = 0) H \Psi_{k,n'}(\phi_0 = 0)$$

$j, k = L, R$

$$\Psi_j^n(r_j, \phi_j) = \langle \vec{r} | j, n \rangle = \psi(r_j) e^{in(\phi_j - \phi_0)}$$

Ring potentials



$$J_{L,n}^{L,-n} = |J_{L,n}^{L,-n}| e^{2in\phi_0} \rightarrow J_1$$

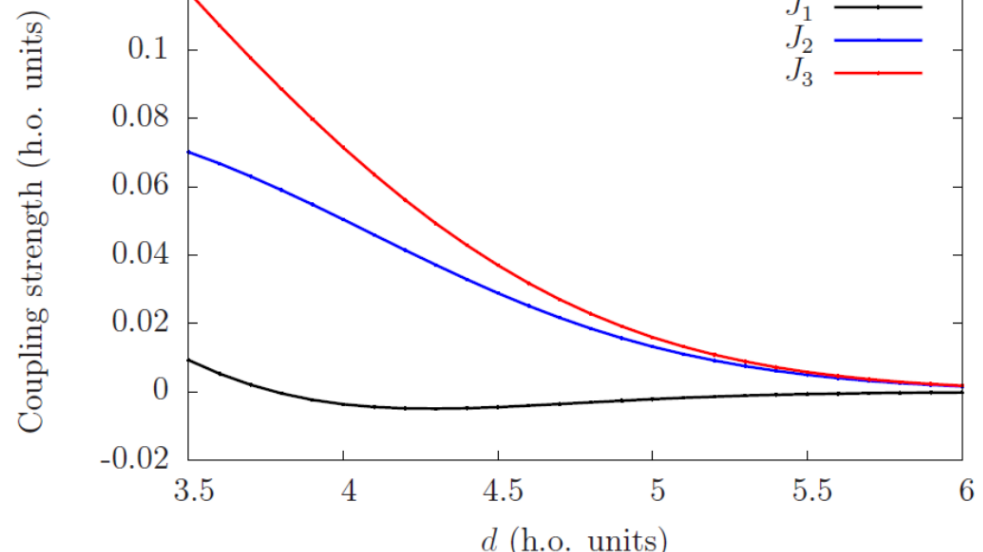
$$J_{L,n}^{R,n} \rightarrow J_2$$

$$J_{L,n}^{R,-n} = |J_{L,n}^{R,-n}| e^{2in\phi_0} \rightarrow J_3$$

J_1 : self coupling

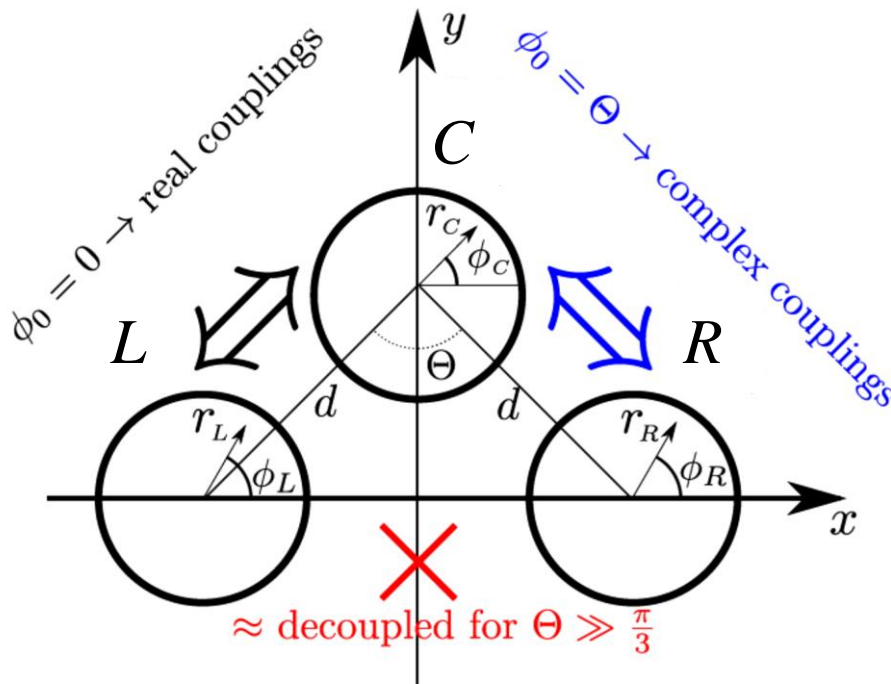
J_2 : cross coupling, no OAM exchange

J_3 : cross coupling, OAM exchange



Ring potentials

J.Polo *et al.*, Phys. Rev. A **93**, 033613 (2016).



Along one direction, $\phi_0 \neq 0 \rightarrow J_1$ and J_3 couplings acquire phases

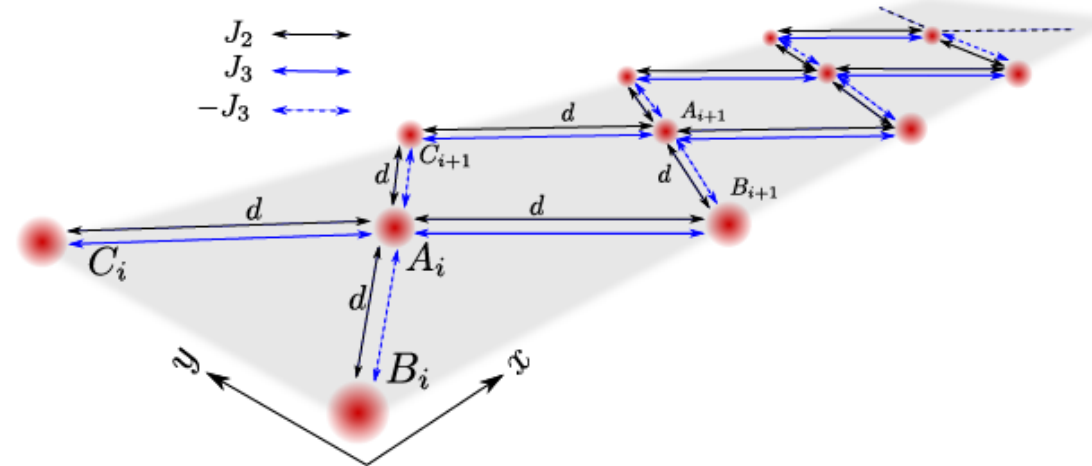
Fast decay of the couplings with $d \rightarrow L$ and R sites decoupled for $\theta \gg \pi/3$

Self-coupling at site C has contributions from L and R sites \rightarrow vanishes for $\theta = \pi/2$

J_1 : self coupling

J_2 : cross coupling, no OAM exchange

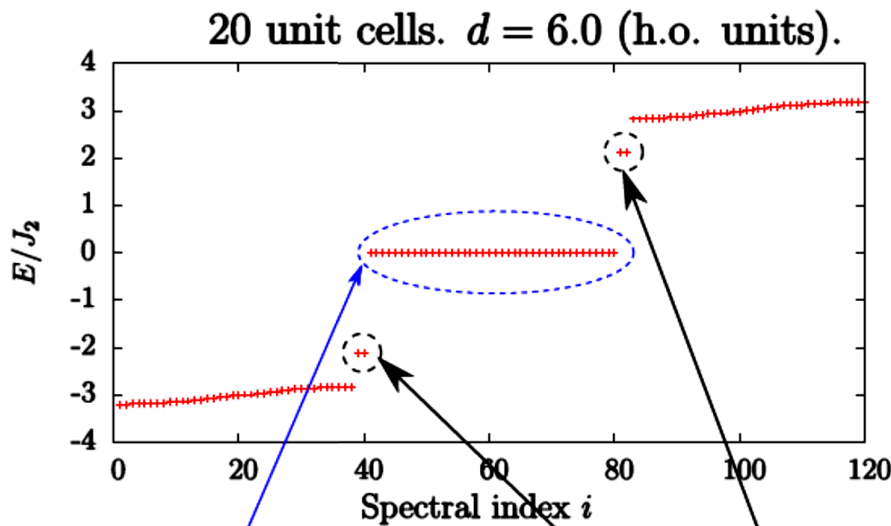
J_3 : cross coupling, OAM exchange



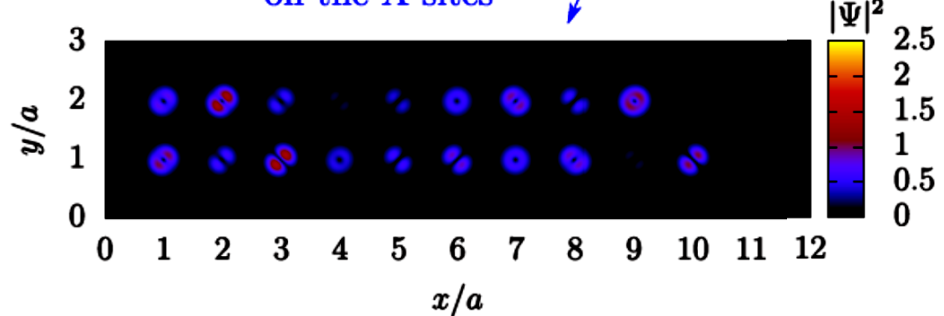
G. Pelegrí *et al.*, Phys. Rev. A **95**, 013614 (2017).

G. Pelegrí *et al.*, Phys. Rev. A **99**, 023612 (2019).

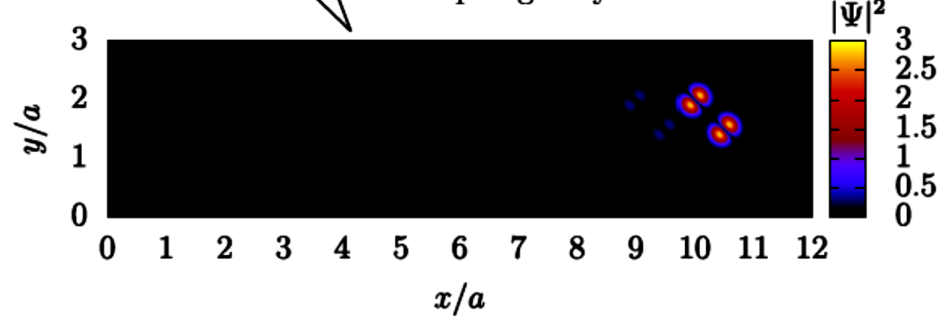
G. Pelegrí *et al.*, Phys. Rev. A **99**, 023613 (2019).



Flat-band states,
with no population
on the A sites



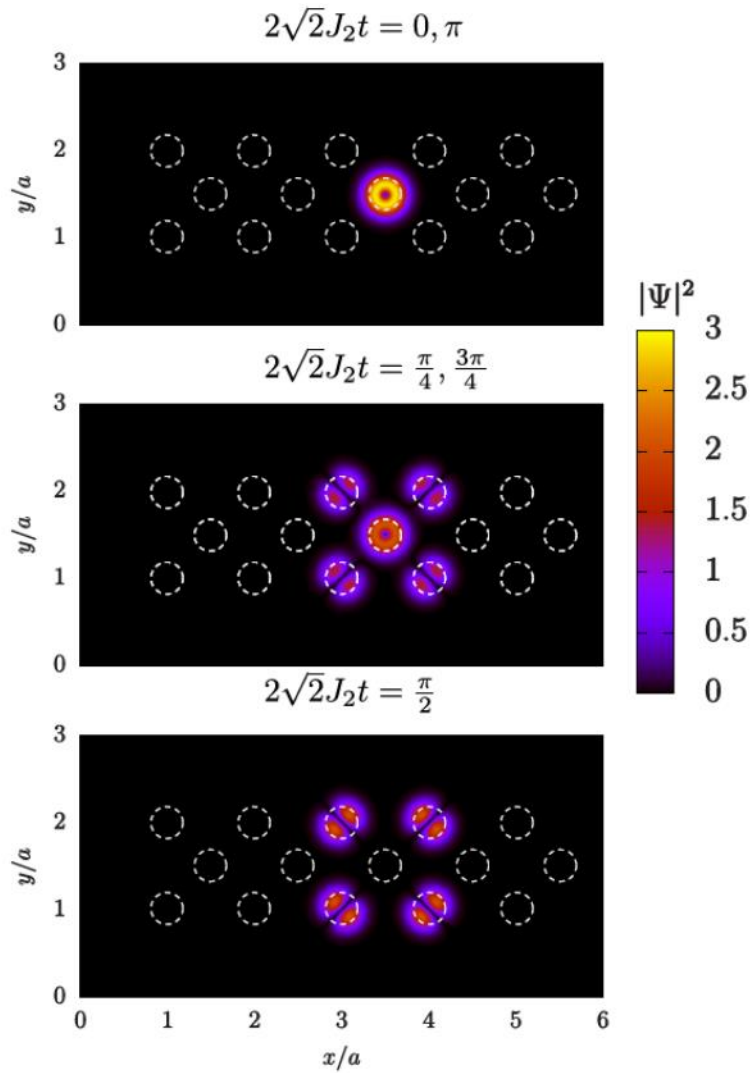
In-gap states,
localized at the right edge
and topologically non-trivial



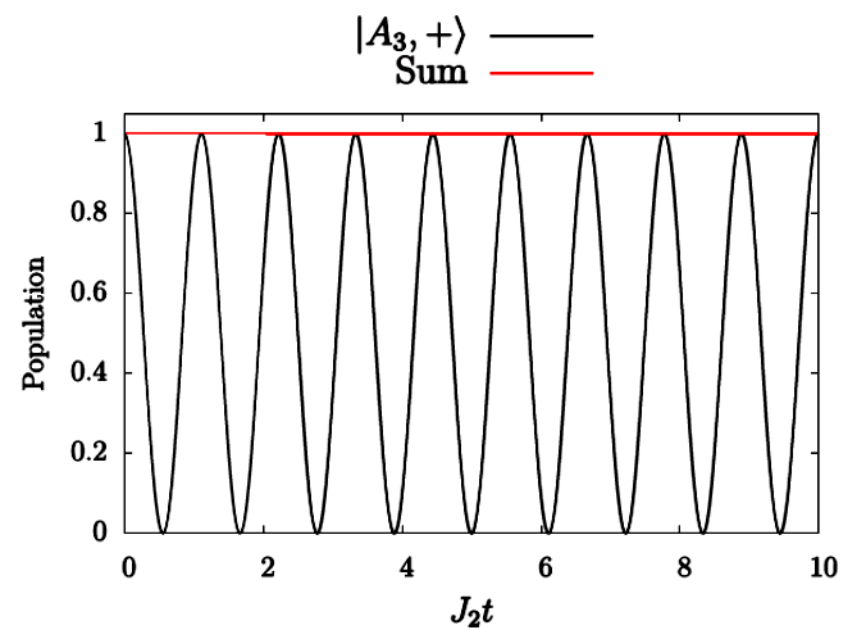
G. Pelegrí *et al.*, Phys. Rev. A **99**, 023612 (2019).

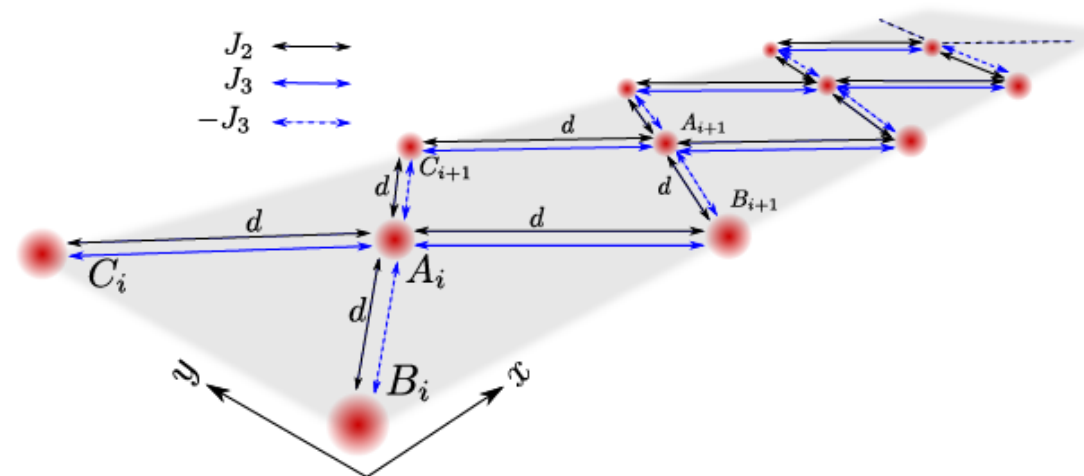
G. Pelegrí *et al.*, Phys. Rev. A **99**, 023613 (2019).

Aharonov-Bohm caging

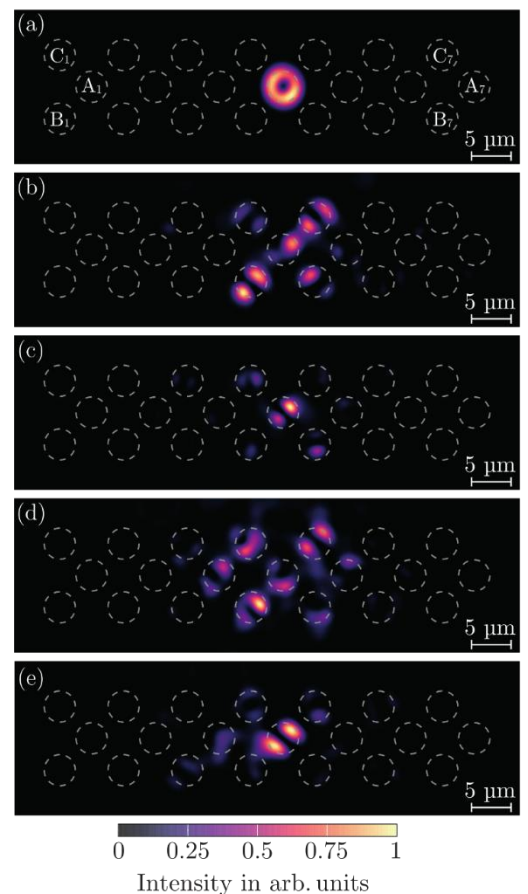


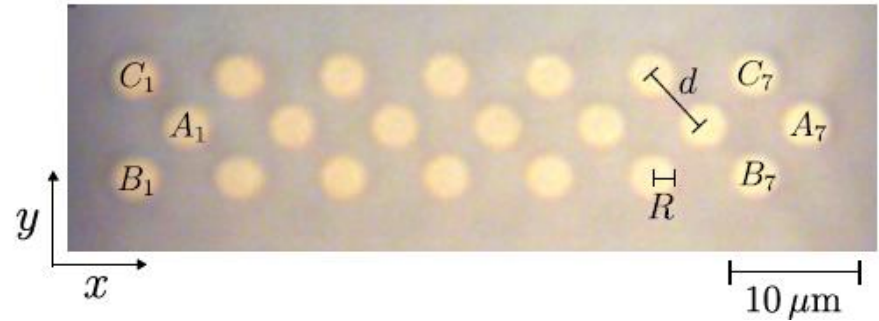
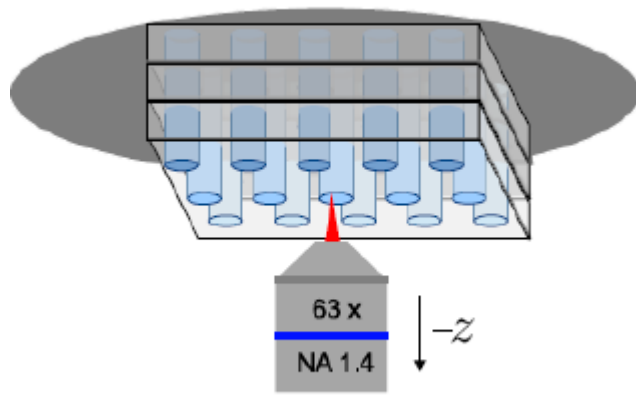
G. Pelegrí *et al.*, Phys. Rev. A **99**, 023612 (2019).
G. Pelegrí *et al.*, Phys. Rev. A **99**, 023613 (2019).





- G. Pelegrí *et al.*, Phys. Rev. A **95**, 013614 (2017).
 G. Pelegrí *et al.*, Phys. Rev. A **99**, 023612 (2019).
 G. Pelegrí *et al.*, Phys. Rev. A **99**, 023613 (2019).

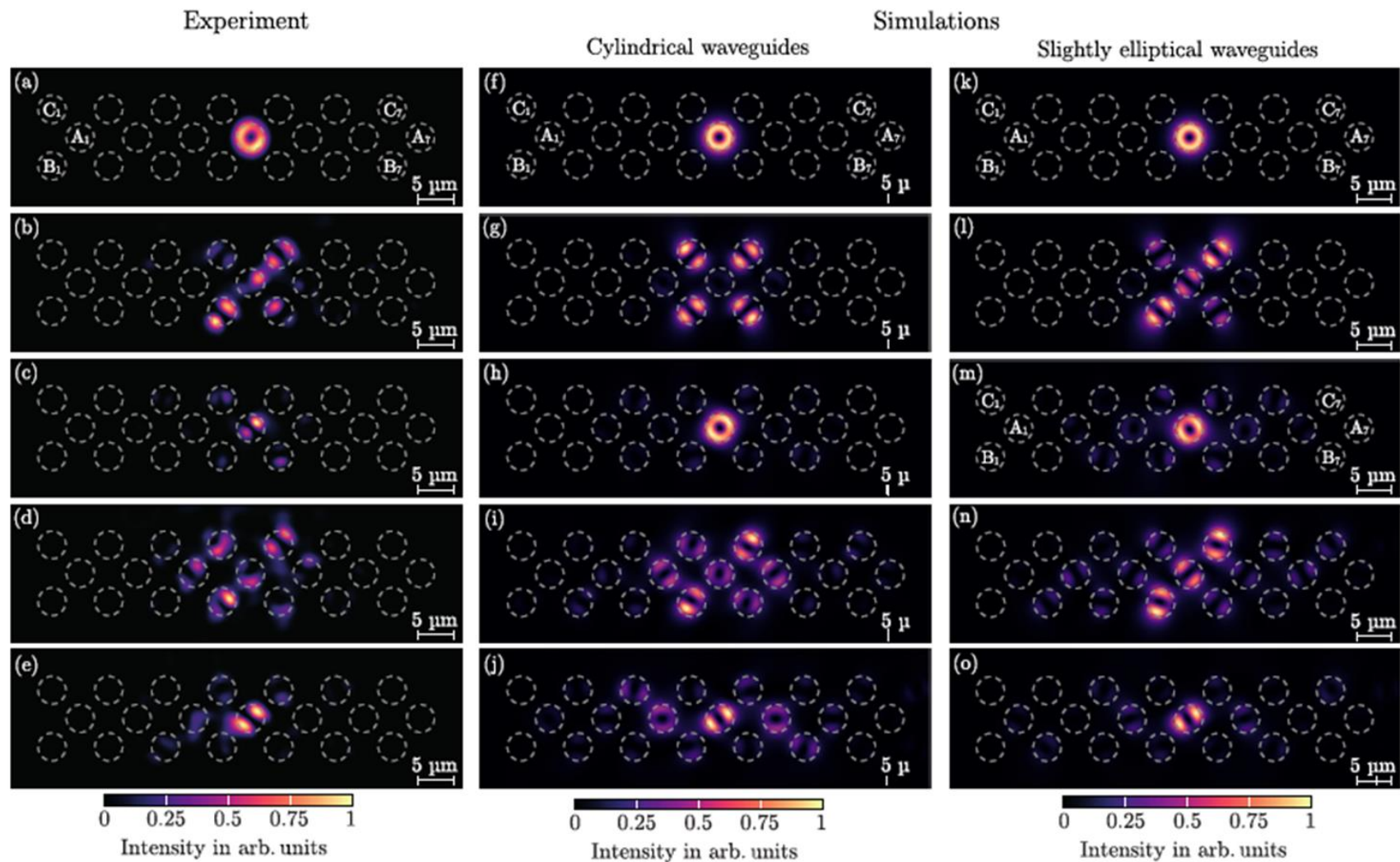




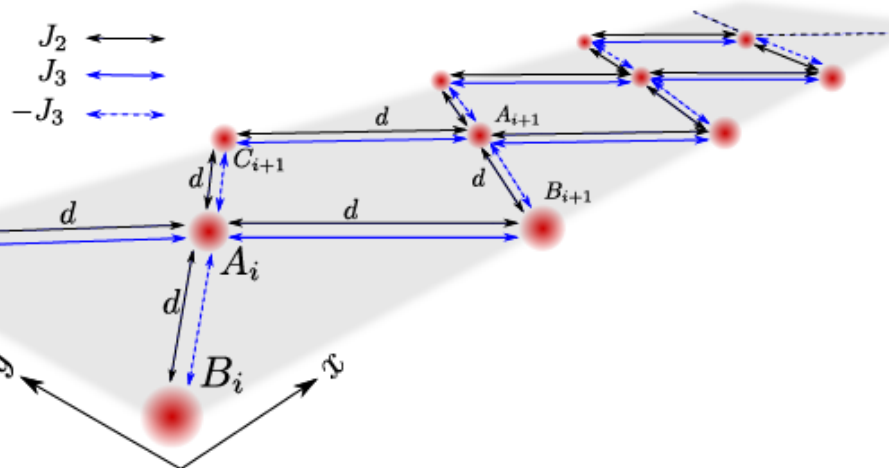
- Nanoscribe system
- Photo resist IP-Dip
- Samples: 0.25-1 mm
- 7 unit cells
- $R = 1.9 \mu\text{m}$
- $\Delta n \sim 0.008$
- $d = 5.5 \mu\text{m}$

C. Jörg, G. Queraltó, M. Kremer, G. Pelegrí, J. Schulz, A. Szameit, G. von Freymann, J. Mompart, V. Ahufinger, *Light Sci Appl* **9**, 150 (2020).

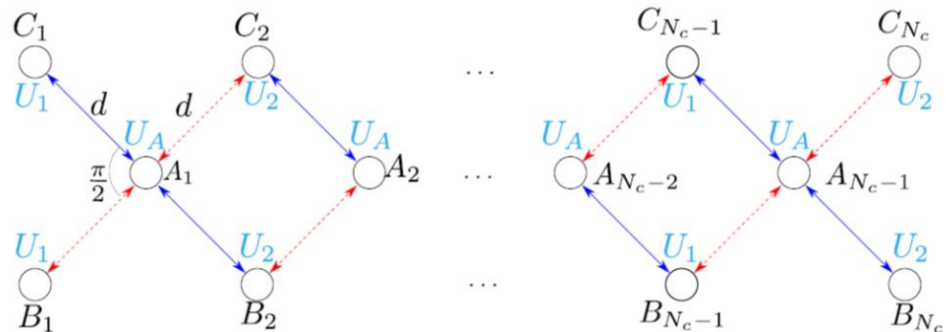
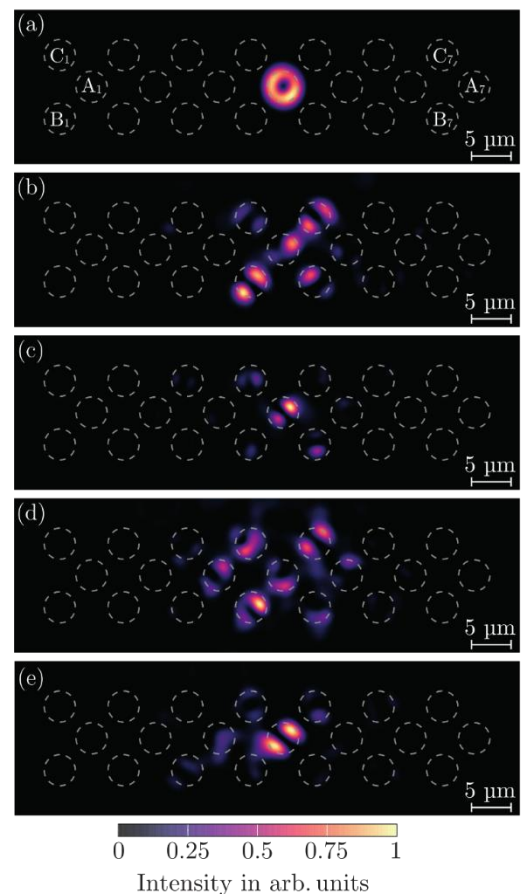
See also: S. Mukherjee et al., *Physical Review Letters* **121**, 075502 (2018).
 M. Kremer et al., *Nature Communications* **11**, 907 (2020).



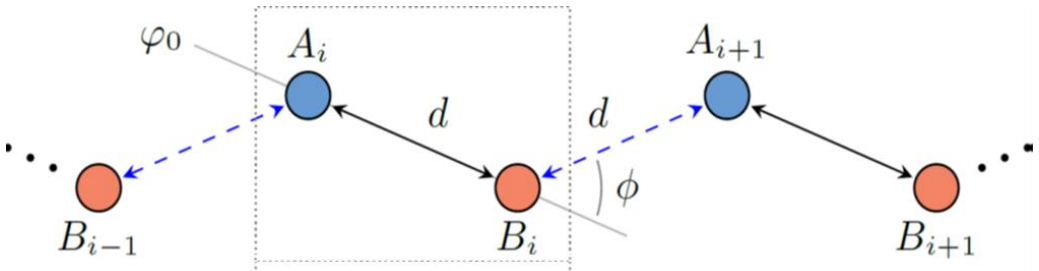
C. Jörg, G. Queraltó, M. Kremer, G. Pelegrí, J. Schulz, A. Szameit, G. von Freymann, J. Mompart, V. Ahufinger, Light Sci Appl 9, 150 (2020).



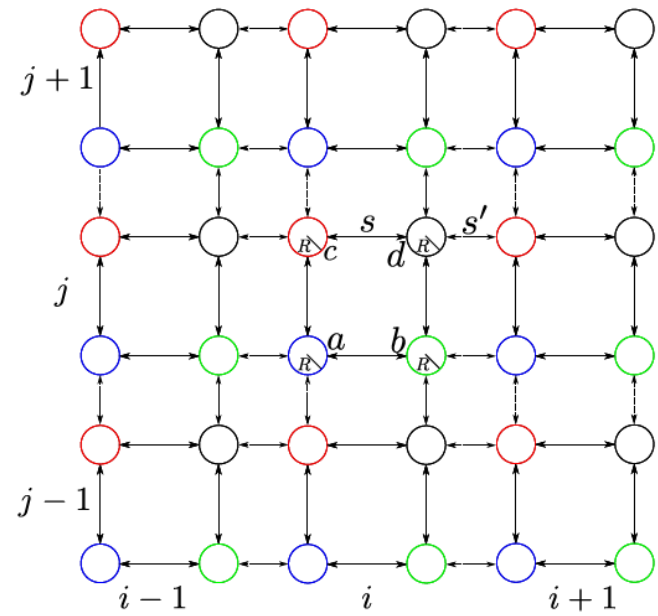
- G. Pelegrí *et al.*, Phys. Rev. A **95**, 013614 (2017).
 G. Pelegrí *et al.*, Phys. Rev. A **99**, 023612 (2019).
 G. Pelegrí *et al.*, Phys. Rev. A **99**, 023613 (2019).



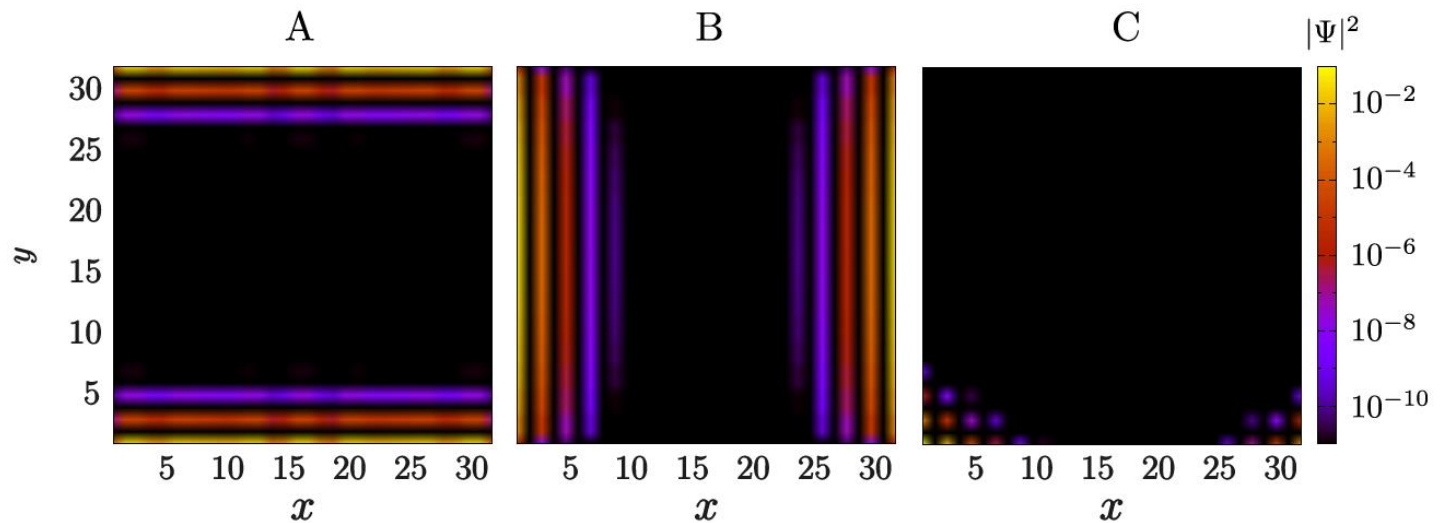
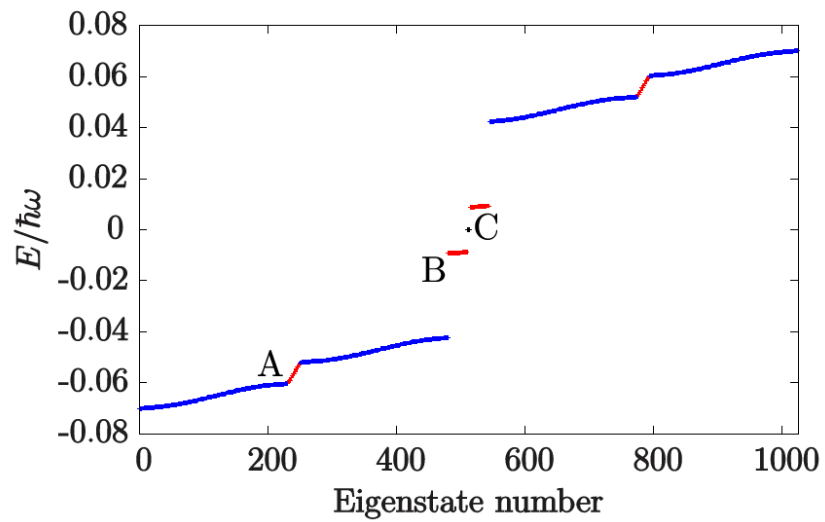
- G. Pelegrí *et al.*, Physical Review Research **2**, 033267 (2020).

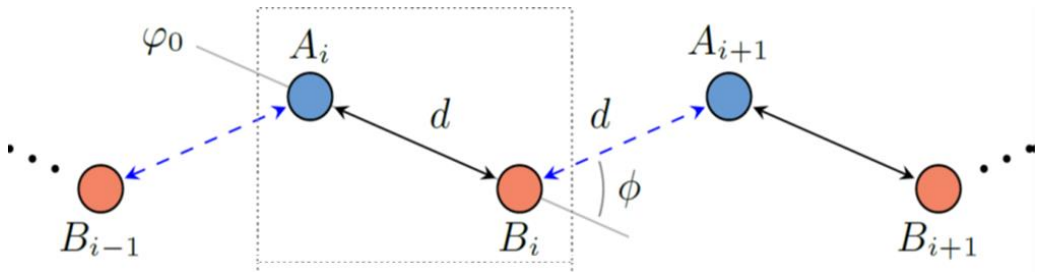


E. Nicolau *et al.*, Phys. Rev. A **107**, 023305 (2023).

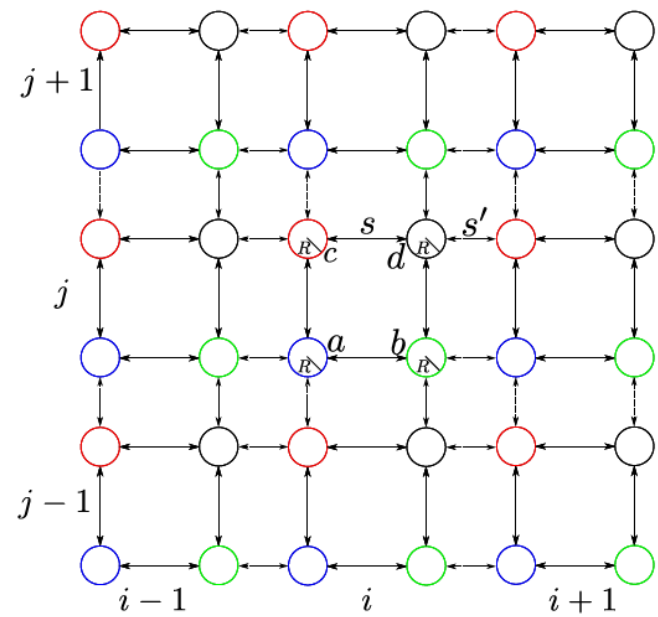


G. Pelegrí *et al.*, Phys. Rev. B **100**, 205109 (2019).





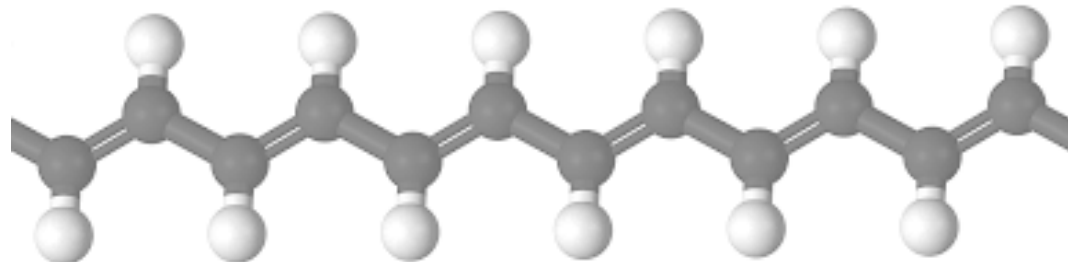
E. Nicolau *et al.*, Phys. Rev. A **107**, 023305 (2023).



G. Pelegrí *et al.*, Phys. Rev. B **100**, 205109 (2019).

E. Nicolau *et al.*, Europhysics Letters **145**, 35001 (2024).

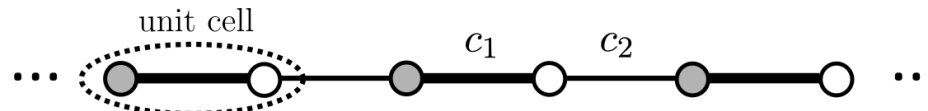
Su-Schrieffer-Hegger model



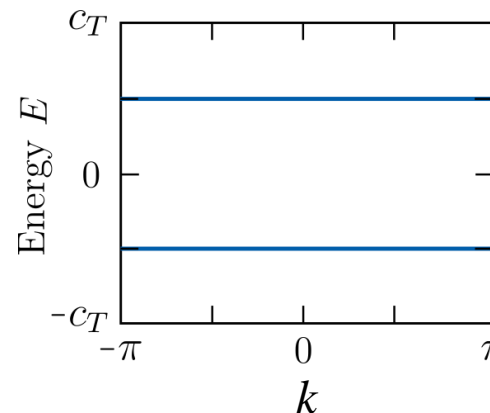
W. P. Su, J. R. Schrieffer, A. J. Heeger, Phys. Rev. Lett. **42**, 1698 (1979).

Su-Schieffer-Hegger model

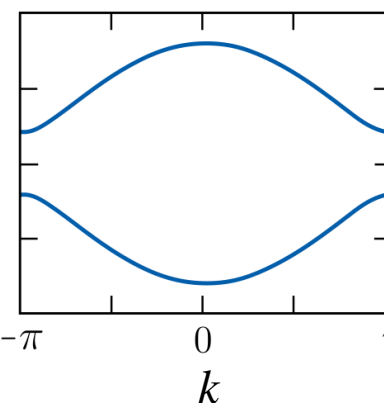
W. P. Su, J. R. Schrieffer, A. J. Heeger, Phys. Rev. Lett. **42**, 1698 (1979).



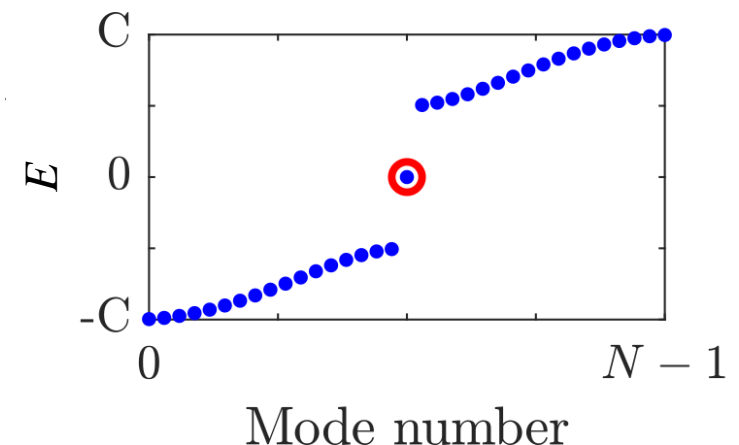
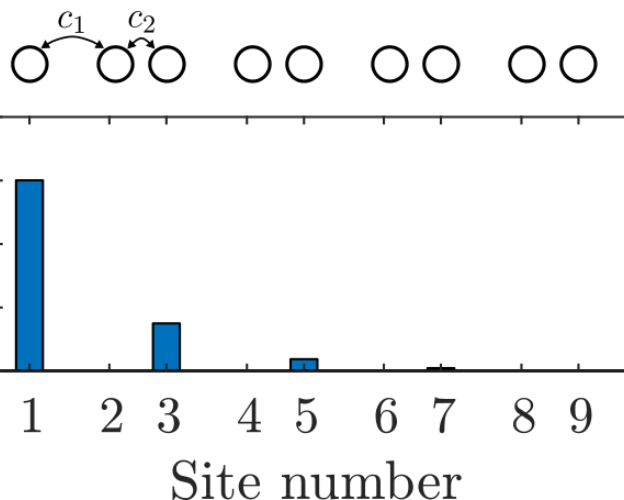
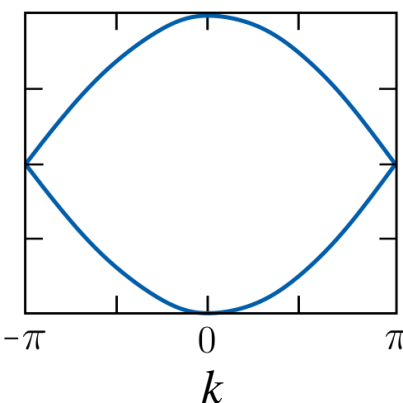
$$c_1 = 0 \text{ or } c_2 = 0$$



$$c_1 \neq c_2$$



$$c_1 = c_2$$



SSH in a lattice of rings

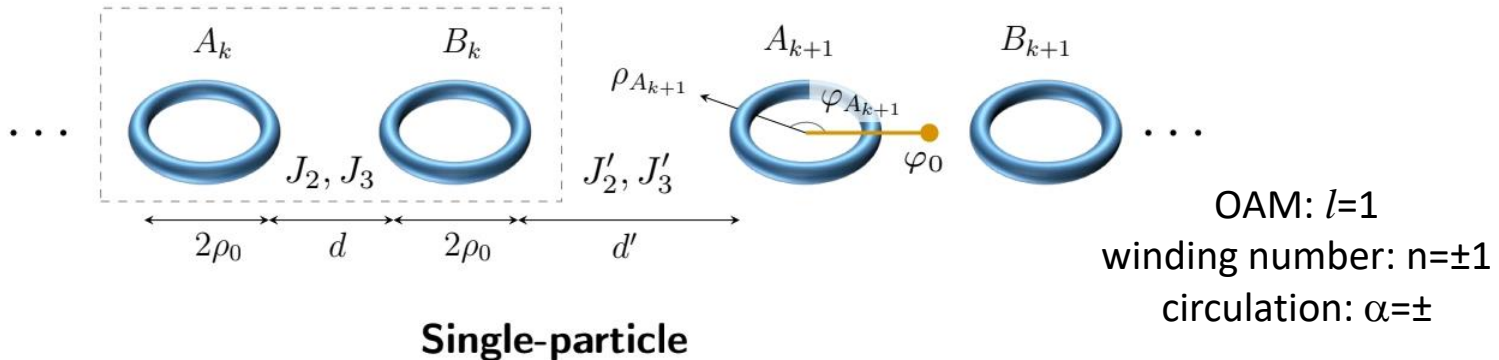


SSH in a lattice of rings

1 atom

E. Nicolau *et al.*, Phys. Rev. A **108**, 023317 (2023).

SSH
structure



$$\hat{\mathcal{H}}_{l=1}^0 = J_2 \sum_{k=1}^{N_c} \sum_{\alpha=\pm} \hat{a}_k^{\alpha\dagger} \hat{b}_k^{\alpha} + J'_2 \sum_{k=1}^{N_c-1} \sum_{\alpha=\pm} \hat{b}_k^{\alpha\dagger} \hat{a}_{k+1}^{\alpha} + J_3 \sum_{k=1}^{N_c} \sum_{\alpha=\pm} \hat{a}_k^{\alpha\dagger} \hat{b}_k^{-\alpha} + J'_3 \sum_{k=1}^{N_c-1} \sum_{\alpha=\pm} \hat{b}_k^{\alpha\dagger} \hat{a}_{k+1}^{-\alpha} + \text{H.c.}$$

Topological characterization

Basis rotation to resolve unitary symmetry

$$\left| A_k^{s(a)} \right\rangle = \frac{1}{\sqrt{2}} (\left| A_k^+ \right\rangle \left(\begin{smallmatrix} + \\ - \end{smallmatrix} \right) \left| A_k^- \right\rangle) \quad \left| B_k^{s(a)} \right\rangle = \frac{1}{\sqrt{2}} (\left| B_k^+ \right\rangle \left(\begin{smallmatrix} + \\ - \end{smallmatrix} \right) \left| B_k^- \right\rangle)$$

$$\left\{ \begin{array}{l} \hat{\mathcal{H}}_s = t_s \sum_{k=1}^{N_c} \hat{a}_k^{s\dagger} \hat{b}_k^s + t'_s \sum_{k=1}^{N_c-1} \hat{a}_{k+1}^{s\dagger} \hat{b}_k^s + \text{H.c.} \\ \hat{\mathcal{H}}_a = t_a \sum_{k=1}^{N_c} \hat{a}_k^{a\dagger} \hat{b}_k^a + t'_a \sum_{k=1}^{N_c-1} \hat{a}_{k+1}^{a\dagger} \hat{b}_k^a + \text{H.c.} \end{array} \right.$$

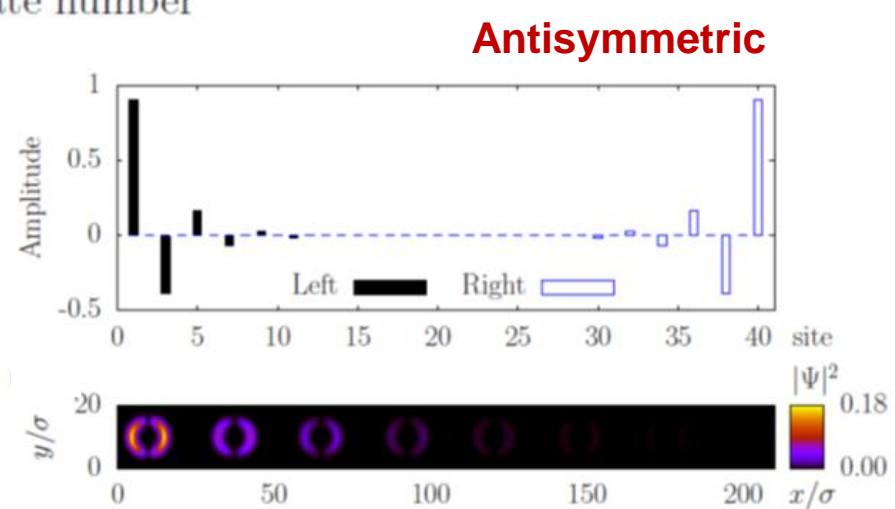
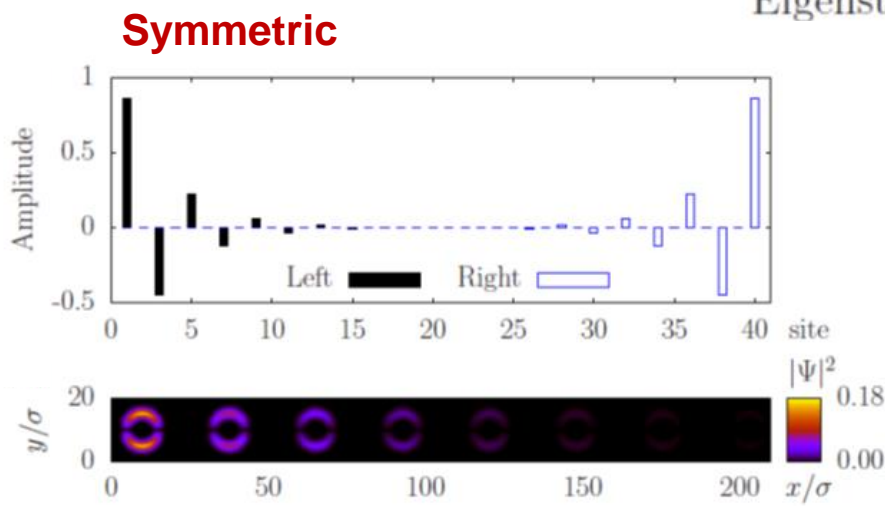
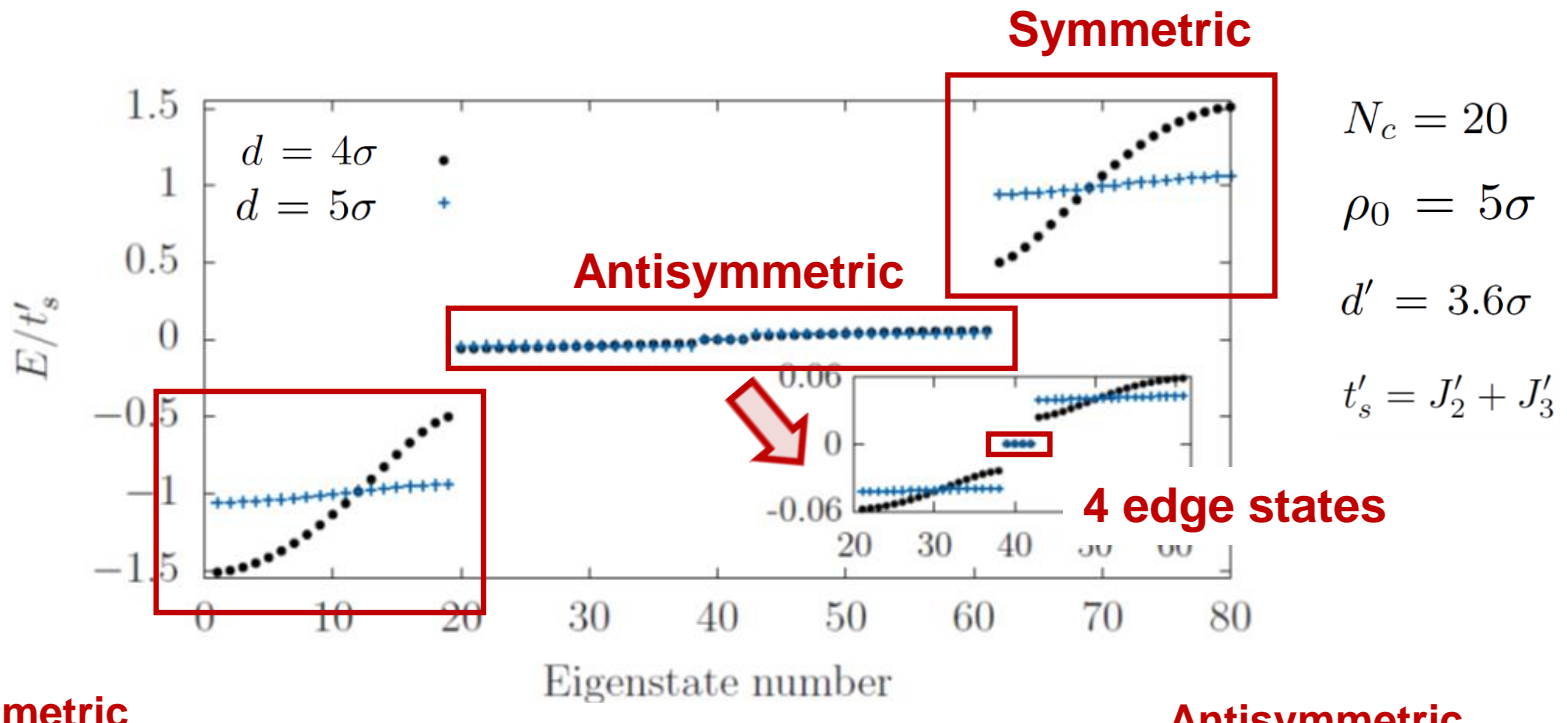
Two decoupled SSH chains

$$t'_a = J'_2 - J'_3, \quad t_a = J_2 - J_3, \\ t'_s = J'_2 + J'_3, \quad t_s = J_2 + J_3.$$

1 atom

SSH in a lattice of rings

E. Nicolau *et al.*, Phys. Rev. A **108**, 023317 (2023).



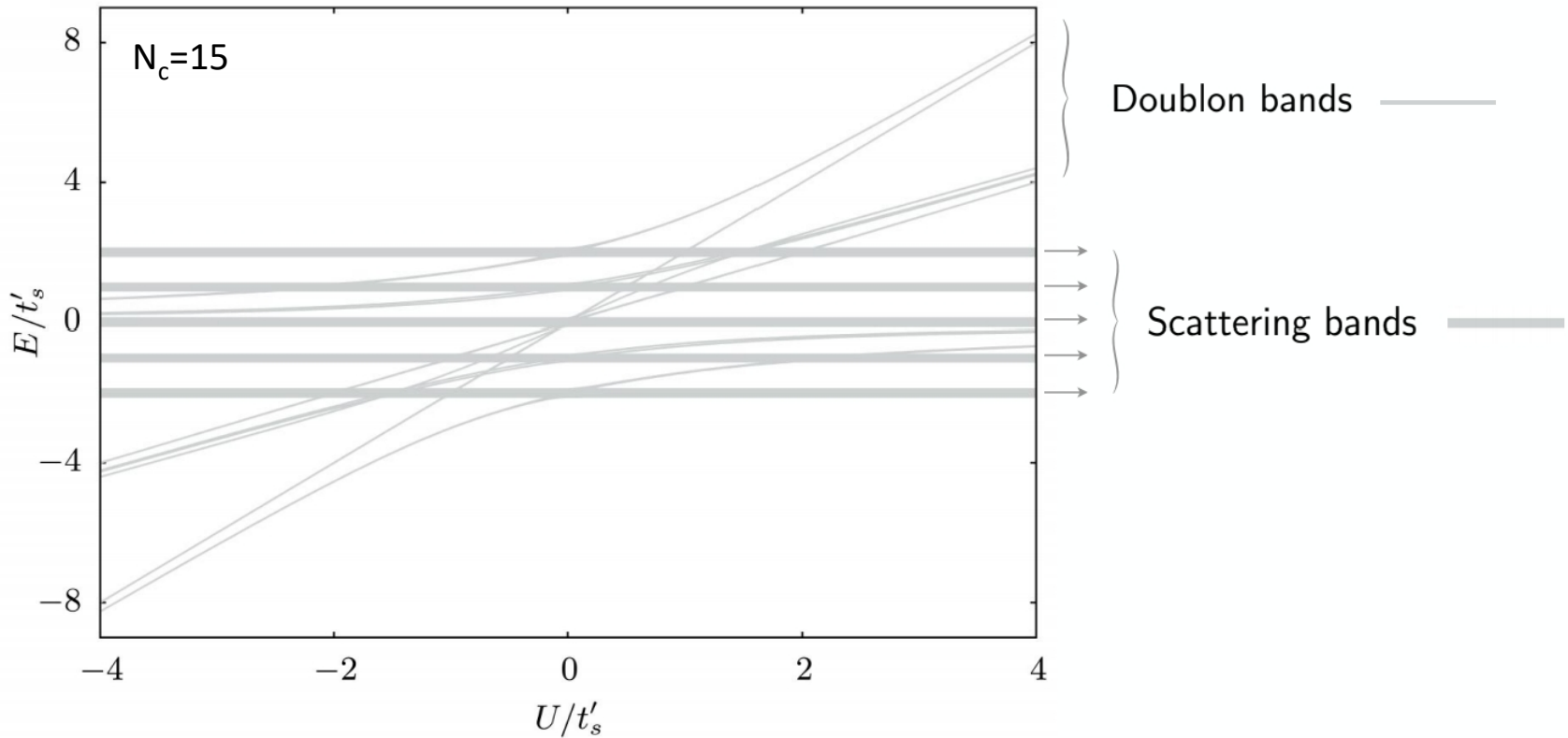
2 atoms

SSH in a lattice of rings

E. Nicolau *et al.*, Phys. Rev. A **108**, 023317 (2023).

On-site boson interactions $\hat{\mathcal{H}}_{l=1}^{int} = \frac{U}{2} \sum_{j=A,B} \sum_{k=1}^{N_c} [\hat{n}_{jk}^+ (\hat{n}_{jk}^+ - 1) + \hat{n}_{jk}^- (\hat{n}_{jk}^- - 1) + 4\hat{n}_{jk}^+ \hat{n}_{jk}^-]$

$$\rho_0 = 5\sigma \quad d = 5\sigma \quad d' = 3.6\sigma$$

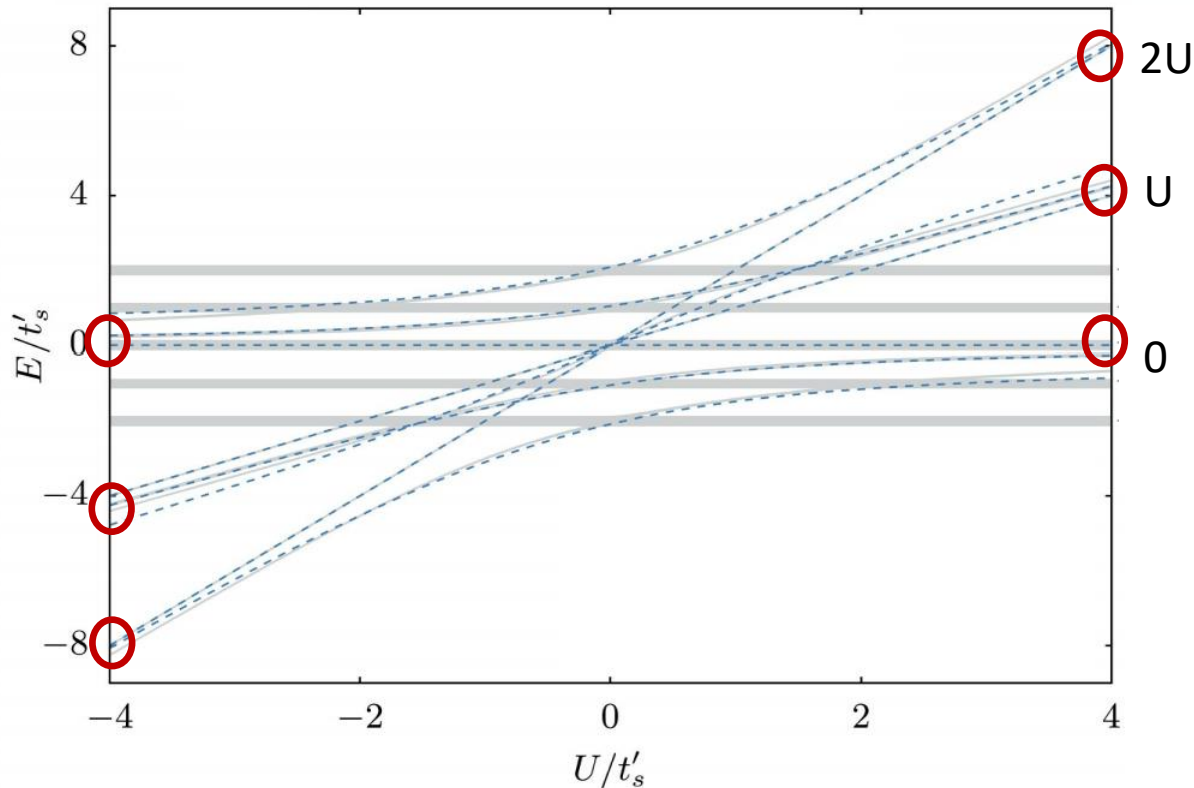


2 atoms

SSH in a lattice of rings

E. Nicolau *et al.*, Phys. Rev. A **108**, 023317 (2023).

strong-link Hamiltonian



strong-link Hamiltonian
(10×10 matrix)



diagonalization

Doublon bands

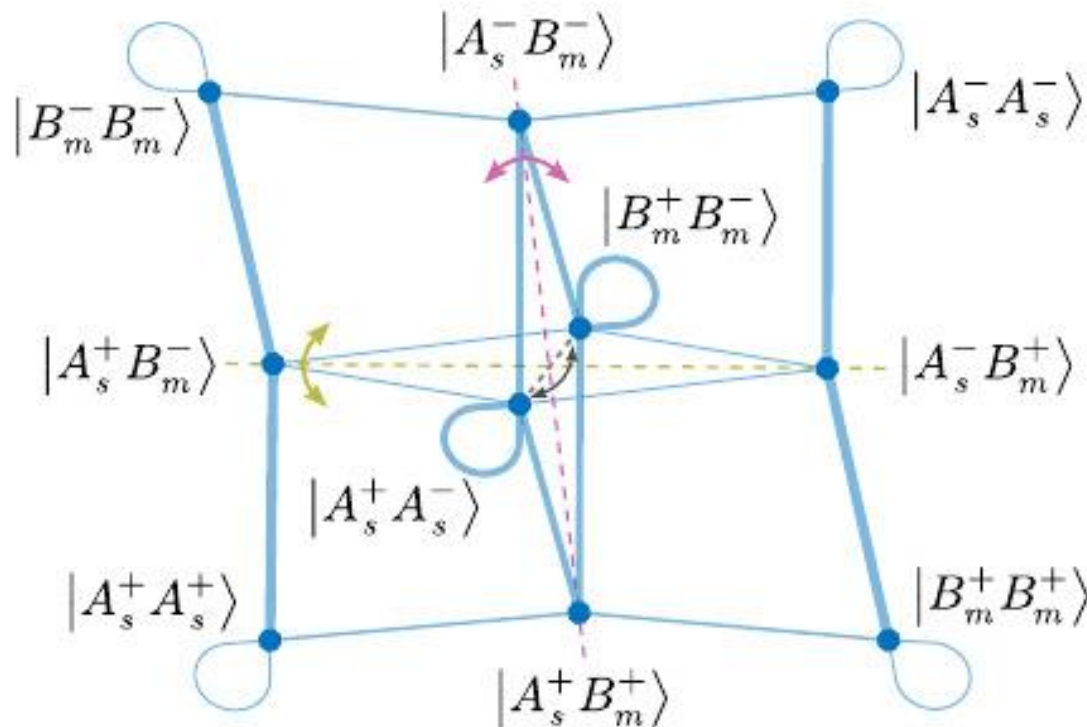


2 atoms

SSH in a lattice of rings

E. Nicolau *et al.*, Phys. Rev. A **108**, 023317 (2023).

strong-link Hamiltonian



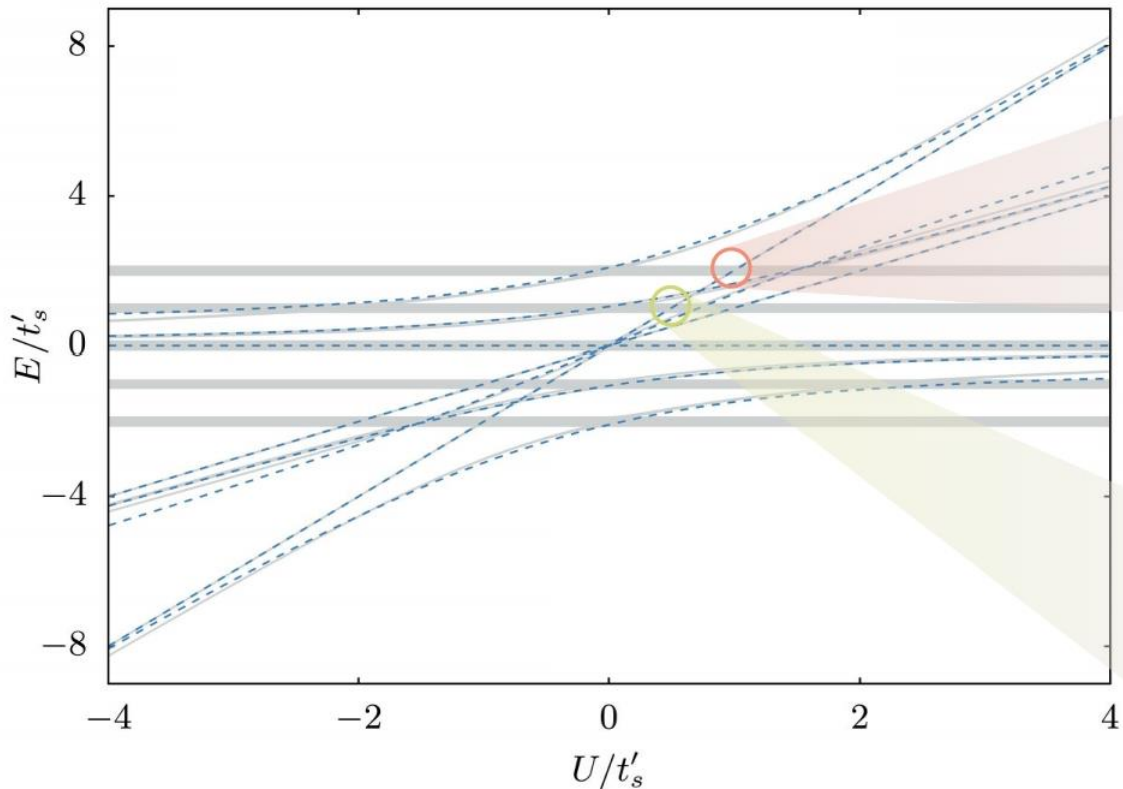
2 atoms

SSH in a lattice of rings

E. Nicolau *et al.*, Phys. Rev. A **108**, 023317 (2023).

strong-link Hamiltonian

Crossings and avoided crossings



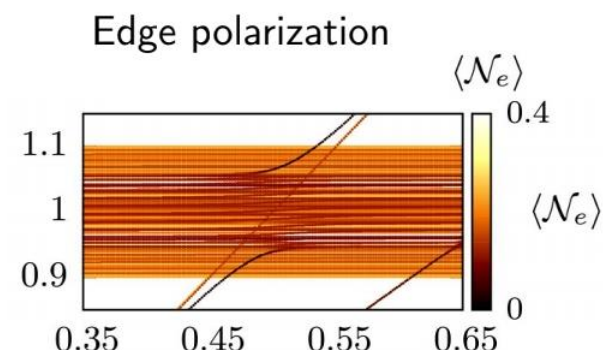
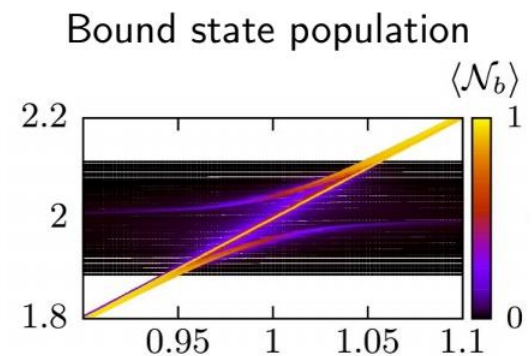
Exchange circulation
symmetry



Well-defined parity



Avoided crossings for states
of the same parity sector



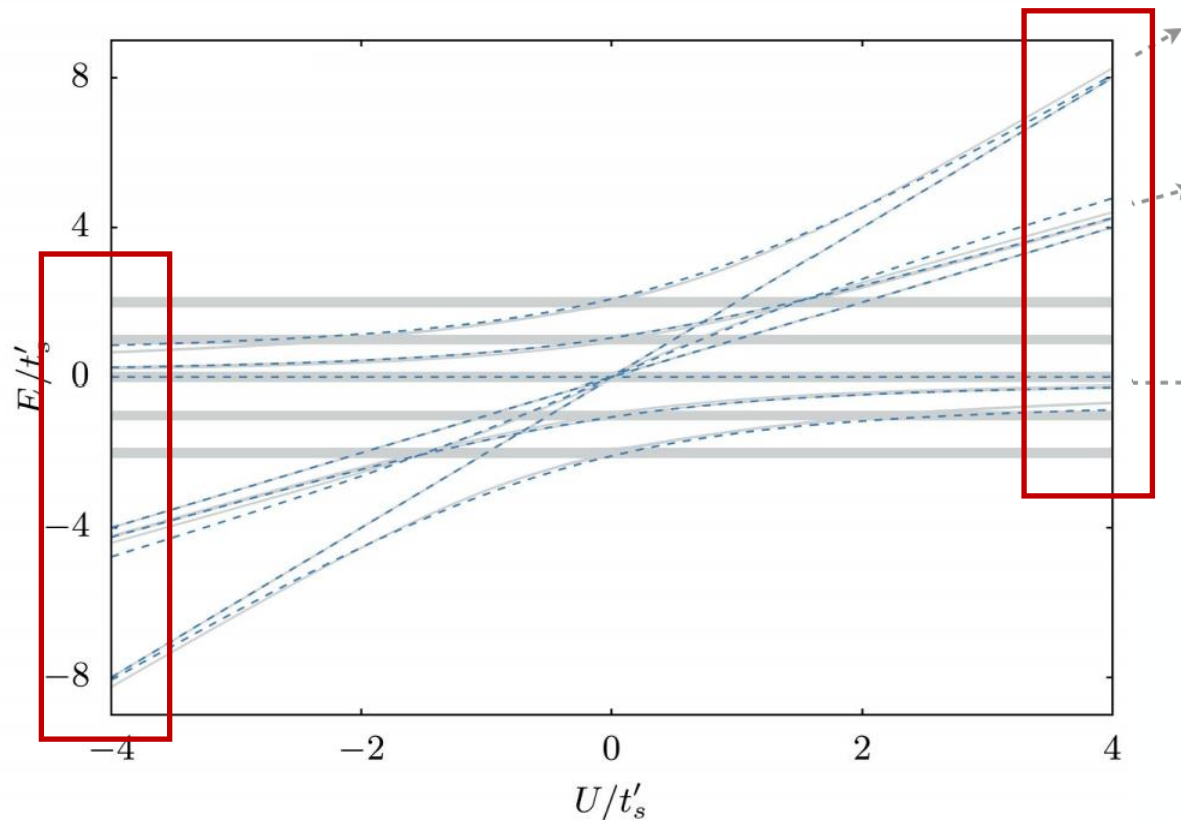
2 atoms

SSH in a lattice of rings

E. Nicolau *et al.*, Phys. Rev. A **108**, 023317 (2023).

strongly interacting limit

Strongly-interacting subspaces $|U| \gg J$



Doublons

\mathcal{B} Opposite circulation

\mathcal{A} Same circulation

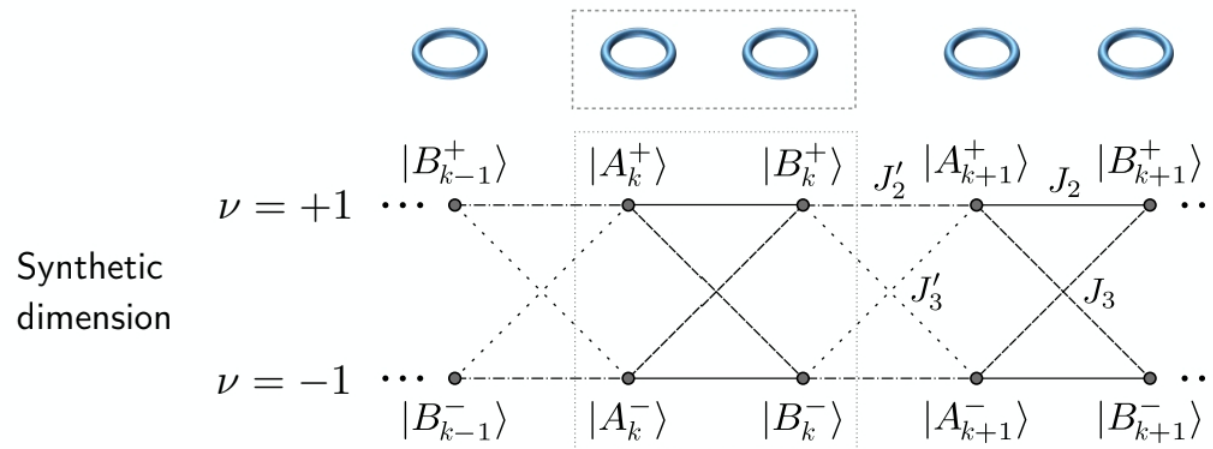
Particles in
different sites

Second order perturbation theory: introduce couplings J as a perturbation

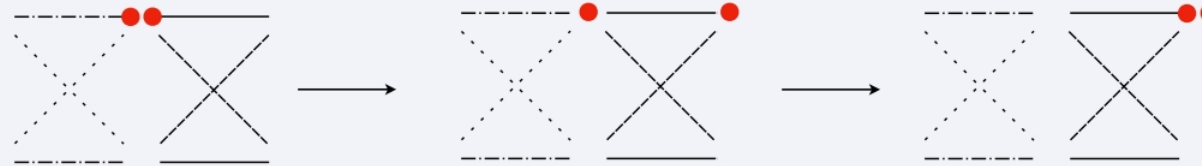
2 atoms

SSH in a lattice of rings

E. Nicolau *et al.*, Phys. Rev. A **108**, 023317 (2023).

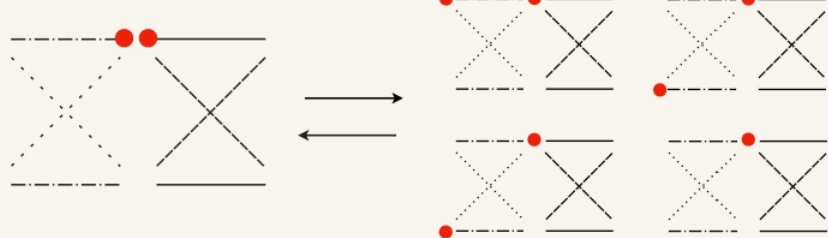


Tunnelings



$$\mathcal{O}\left(\frac{J^2}{U}\right)$$

On-site potential



$$\mathcal{O}\left(\frac{J^2}{U}\right)$$

Bulk-edge on-site potential mismatch

2 atoms

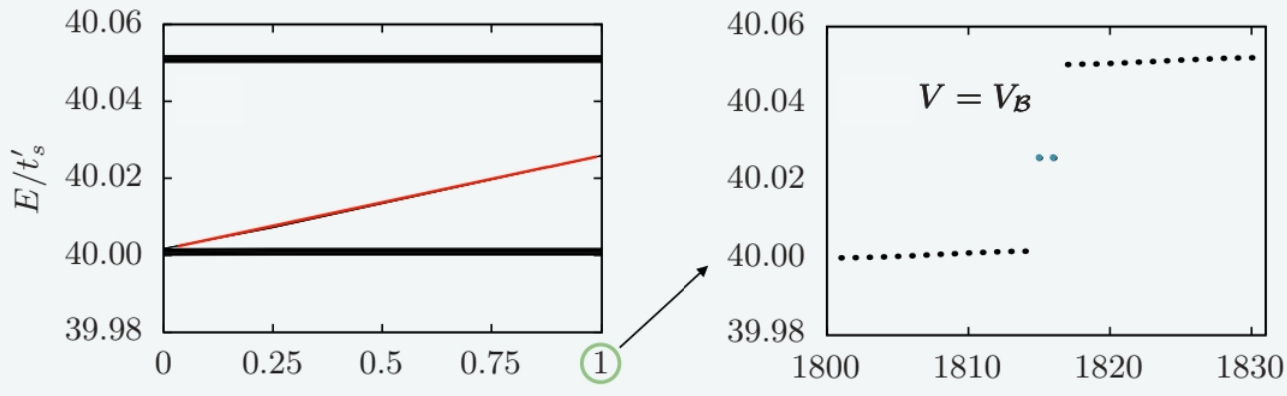
SSH in a lattice of rings

E. Nicolau *et al.*, Phys. Rev. A **108**, 023317 (2023).

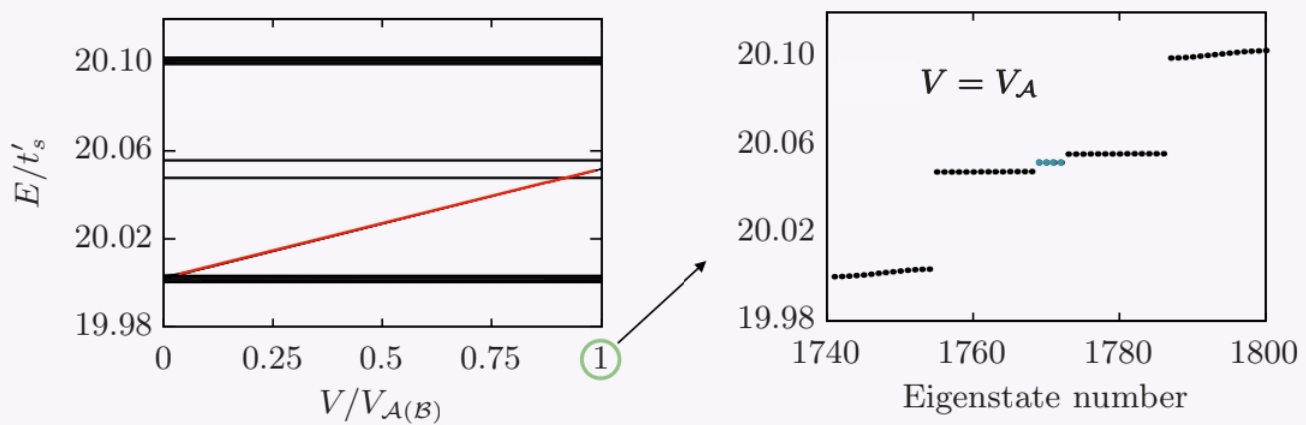
strongly interacting limit

Effective single-particle models

\mathcal{B}
SSH chain



\mathcal{A}
Creutz
ladder



edge potential correction

Tamm-Shockley states

(chiral symmetry, quantized Zak phase)

Topologically protected edge states

Conclusions

Ultracold atoms carrying orbital angular momentum in lattices constitute a novel platform to explore topology for single atoms and interacting few-atoms systems.

As an example...



Single particle we have characterized the model topologically through an exact mapping.

Two particles we have analyzed the interplay between interactions and topology in the dimerized limit, in terms of a strong-link Hamiltonian, and in the strongly interacting limit, by means of perturbation theory.

**Thank you for your
attention**